Combustion Science and Technology

ISSN: (Print) (Online) Journal homepage: www.tandfonline.com/journals/gcst20

Numerical Investigation of Hydrogen Role on Detonation of CH_4/H_2/air Mixtures

Chenyuan Cai, Min Li, Kaiqiang Jin & Huahua Xiao

To cite this article: Chenyuan Cai, Min Li, Kaiqiang Jin & Huahua Xiao (22 Jul 2024): Numerical Investigation of Hydrogen Role on Detonation of CH_4/H_2/air Mixtures, Combustion Science and Technology, DOI: 10.1080/00102202.2024.2382252

To link to this article: https://doi.org/10.1080/00102202.2024.2382252

Published online: 22 Jul 2024.

Submit your article to this journal

View related articles

View Crossmark data

Full Terms & Conditions of access and use can be found at
https://www.tandfonline.com/action/journalInformation?journalCode=gcst20

COMBUSTION SCIENCE AND TECHNOLOGY
https://doi.org/10.1080/00102202.2024.2382252

Numerical Investigation of Hydrogen Role on Detonation of CH_4/H_2/air Mixtures

Chenyuan Cai, Min Li, Kaiqiang Jin, and Huahua Xiao

State Key Laboratory of Fire Science, University of Science and Technology of China, Hefei, China

ABSTRACT

Steady one-dimensional Zeldovich-von Neumann-Döring (ZND) calculation and thermo-chemical analysis are performed to investigate the hydrogen role on ZND detonation of CH_4/H_2/air mixtures. Different hydrogen blend ratios (i.e. *Hbr*) ranging from 0% to 100% are selected in this paper. The results show that hydrogen blend ratio has a significant impact on the ZND detonation reaction pathway of stoichiometric CH_4-air mixtures. When $Hbr \leq 20\%$, CH_4 is converted to CO_2 by route 1: $CH_4 => CH_3 => C_2H_6 => \ldots => CO_2$ and route 2: $CH_4 => CH_3 => CH_3O => CH_2O => HCO => CO => CO_2$. When $Hbr \geq 50\%$, CH_3 in route 2 is directly converted to CH_2O through R97 ($CH_3 + O <=> CH_2O + H$). This causes different ZND detonation structures. The induction length decreases with hydrogen addition. This is because R0 ($H + O_2 <=> O + OH$) governs the heat release during the induction stage, enhancing the energy absorption in induction stage and the molecular thermal decomposition after leading shock wave. Finally, the effect of hydrogen blend ratio on the detonation cell size is explored, and a prediction model of detonation cell size incorporated with detonation stability parameter and induction length is developed for CH_4/H_2/air mixtures.

ARTICLE HISTORY
Received 1 April 2024
Revised 1 June 2024
Accepted 15 July 2024

KEYWORDS
CH_4/H_2/air mixture; ZND detonation; reaction pathway; induction length; detonation cell size

Introduction

Nowadays, the world energy consumption is still dominated by the fossil fuels like coal and oil. The use of these fossil energy sources has been causing pollutions to the environment on which humans rely for survival. To address this issue, hydrogen has attracted considerable attention as a fuel candidate because of its high energy efficiency and clean combustion characteristics (Midilli et al. 2005). However, the properties of hydrogen in connection with ultra-low ignition energy, broad flammable range, faster laminar burning velocity, wide explosion limit, and high diffusivity, pose significant challenges to its transportation and storage (Ng and Lee 2008; Xiao, Duan, and Sun 2018). An efficient way to transport and use hydrogen fuel is blending it into existing natural gas (Cai et al. 2023; Mejía-Botero, Veiga-López, and Melguizo-Gavilanes 2022; Ogden et al. 2018; Oran, Gamezo, and Zipf 2015) or ammonia (Li and Xiao 2023a, Li and Xiao 2023b; Li, Xiao, and Sun 2022).

The binary fuel containing methane and hydrogen is regarded as an important means of hydrogen utilization. The combustion characteristics of CH_4-H_2 mixtures have been

CONTACT Min Li lim2010@ustc.edu.cn State Key Laboratory of Fire Science, University of Science and Technology of China, No. 443 Huangshan Road Shushan District, Hefei 230027, China; Huahua Xiao xiaoh@ustc.edu.cn State Key Laboratory of Fire Science, University of Science and Technology of China, No. 443 Huangshan Road Shushan District, Hefei 230027, China

© 2024 Taylor & Francis Group, LLC

studied experimentally and numerically, which contribute to a better understanding of the combustion behaviors. Laminar burning velocity is one of the most important combustion properties. The velocity was found to increase with the hydrogen fraction in fuel mixture (de Goey, Hermanns, and Bastiaans 2007; Huang et al. 2006; Pio and Salzano 2018; Yu, Law, and Wu 1986). Further exploration indicated that the increase of laminar burning velocity by hydrogen addition is associated with the overall activation energy (Cheng, Tang, and Huang 2015; de Goey, Hermanns, and Bastiaans 2007), adiabatic flame temperature (Cheng, Tang, and Huang 2015), inner layer temperature (de Goey, Hermanns, and Bastiaans 2007; Zhang et al. 2016), and global Lewis number (Cheng, Tang, and Huang 2015). Based on the laminar burning velocity, many premixed flame phenomena such as flashback, extinction, and flame propagation can be characterized, and the chemical kinetics mechanisms are able to be validated or simplified (Okafor et al. 2018). Although the reduced mechanisms have been developed by Sher et al. (1988) and Gimeno-Escobedo et al. (2019), the chemical kinetics of hydrogen addition on methane or natural gas chemical reaction process were not well understood. In this context, Wang et al. (2009) investigated the chemical kinetics effect of hydrogen on stoichiometric CH_4/H_2/air mixtures by performing the one-dimensional (1D) numerical simulations of premixed laminar flames. They discovered that the role of hydrogen in the flame changes from intermediate species to reactant when the hydrogen fraction in the blends exceeds 20%. The result that hydrogen is an important intermediate in hydrocarbon-air flames was also found by He et al. (2020).

In addition to the basic combustion properties of CH_4-H_2 binary fuels, the explosion characteristics such as overpressure have been examined (Cai et al. 2022; Liu et al. 2021; Mitu et al. 2020). Su et al. (2021) further evaluated the chemical kinetic behaviors at the chain initiation stage of CH_4/H_2/air mixtures explosion process using the density functional theory. They concluded that methane is crucial for the chain initiation stage, while hydrogen plays a more important role than methane after the chain reaction begins. Takita and Niioka (1996) explored the detonation of CH_4-H_2 and CH_4-C_4H_{10} mixtures by measuring the detonation velocity. They found that the mixture with a lower sensitivity (e.g., CH_4-air mixtures) can be considerably reduced by adding a small amount of another fuel with a higher sensitivity, such as hydrogen and butane. Similar results were also obtained by Bozier et al. (2009). They discovered that adding hydrogen to natural gas promotes its detonability and the mixtures are more sensitive than heavy alkane-air mixtures when the hydrogen molar fraction exceeds 0.65. Recently, more detonation characteristics such as velocity deficit or fluctuation (Li et al. 2022; Porowski and Teodorczyk 2013), pressure (Li, Hampp, and Lindstedt 2015; Rudy, Zbikowski, and Teodorczyk 2016; Shamshin et al. 2021), induction length (Zhang 2019; Zhang, Pang, and Gao 2016), detonation cell size (Mejía-Botero, Veiga-López, and Melguizo-Gavilanes 2022; Rodriguez et al. 2022; Zhang, Pang, and Gao 2016), and run-up distance (Shamshin et al. 2021; Sorin et al. 2009; Bozier et al. 2009) as well as run-up time (Shamshin et al. 2021) to deflagration-to-detonation transition in CH_4-H_2 fuel blends have been analyzed. Furthermore, the detonation behaviors, including the detonation limits (Zhang, Pang, and Gao 2016), detonation stability (Zhang, Pang, and Gao 2016), and critical conditions (Mejía-Botero, Veiga-López, and Melguizo-Gavilanes 2022; Sun and Lu 2020a, Sun and Lu 2020b) were assessed. Chaumeix et al. (2007) experimentally measured the auto-ignition delay times of hydrogen/natural gas/air mixtures.

It can be found most researchers paid more attention to the macroscopic parameters of the detonation of CH_4-H_2 mixtures, and less attention to the variation of the detonation properties from the perspective of chemical kinetics. Existing studies are not enough to understand the detailed detonation phenomenon. The internal reaction mechanism of the changes in the detonation influenced by the hydrogen blend ratio of CH_4/H_2/air mixtures still needs to be further explored. Zeldovich, von Neumann, Döering (ZND) detonation model provides both the ignition and the driving mechanisms for the detonation wave. This is an important model where the detailed chemical kinetics of the explosive reactions can be studied under the gas dynamics conditions corresponding to the detonation process. The analysis of the laminar structure of ZND detonation also provides a characteristic chemical length scale (e.g., induction length) for the detonation, which can be correlated with real detonation parameters (e.g., detonation cell size).

The objective of this work is to investigate the hydrogen blend ratio on ZND detonations of CH_4/H_2/air mixtures. This is conducted through numerical simulations by using the steady 1D ZND calculation and thermo-chemical analysis. Different hydrogen blend ratios (ranging from 0–100%) were considered in the simulations to explore the hydrogen role on the ZND detonations, including the detonation structure, induction length, and detonation cell size.

Method

ZND detonation solver

The ZND theory is used to describe the dynamics of 1D steady planar detonation. For the shock-attached frame, the evolution of the system along the path of a Lagrangian particle (zero-dimensional problem) is described using:

$$\eta \frac{dv}{dt} = v\dot{\sigma}, \tag{1}$$

$$\eta \frac{d\rho}{dt} = -\rho\dot{\sigma}, \tag{2}$$

$$\eta \frac{dP}{dt} = -\rho v^2 \dot{\sigma}, \tag{3}$$

$$\frac{dy_k}{dt} = \frac{W_k}{\rho}\dot{\omega}_k, \tag{4}$$

$$\dot{\sigma} = \sum_{k=1}^{N} \left(\frac{\bar{W}}{W_k} - \frac{h_k}{c_p T}\right)\frac{\dot{\omega}_k}{\rho}, \tag{5}$$

$$\eta = 1 - Ma^2, \tag{6}$$

where t is the time, v is the velocity, ρ is the density, P is the pressure, $\dot{\sigma}$ is the thermicity (i.e., the non-dimensional energy release rate), η is the sonic parameter, Ma is the Mach number, N is the species number, $\bar{W}$ is the mean molar mass, c_p is the heat capacity at constant pressure, T is the temperature, y_k, $\dot{\omega}_k$, h_k, and W_k are the mass fraction, source term, enthalpy, and molecular weight, respectively. The governing equations are solved using Cantera (Goodwin, Moffat, et al. 2022) as well as the Shock and Detonation Toolbox (Browne et al. 2018). The numerical method has been extensively used and tested in the studies, including the detonation in NH_3-O_2 and NH_3-N_2O mixtures (Weng, Mével, and Chaumeix 2023), the effect of ozone addition on curved detonations (Weng et al. 2023), the real gas effect on the steady planar detonation (Weng and Mevel 2022), and so on (Kumar, Ivin, and Singh 2021; Sun, Tian, and Chen 2022).

The detonation process of the mixtures is described by the Foundational Fuel Chemistry Model 1.0 (FFCM-1) (Tao, Smith, and Wang 2018). This detailed chemical reaction mechanism is composed of 291 reactions and 38 species, which has been validated by numerous basic experimental data of small hydrocarbon fuels (Liu et al. 2021; Tao, Smith, and Wang 2018), e.g., H_2-CO, CH_4, CH_2O, CH_3OH, and C_2H_4. The mixtures applied in this study are stoichiometric CH_4/H_2/air mixtures with various hydrogen blend ratios initially at 298 K and 101,325 Pa, as follows:

$$(1 - x_{H_2})CH_4 + x_{H_2}H_2 + \frac{4 - 3x_{H_2}}{2}(O_2 + 3.76N_2) \Rightarrow \mathrm{Pr\,oducts}, \tag{7}$$

where x_{H_2} is the molar fraction of hydrogen in the fuel (i.e., $Hbr = 0\%$, 20%, 50%, 80%, and 100%).

Thermo-chemical analysis

The state of mixtures at every time is available from the solution of the ZND model. Accordingly, the rate of production, the heat release rate, and the sensitivity coefficient can be calculated. The methods are as follows (Li, Weng, and Mével 2022; Weng, Mével, and Chaumeix 2023):

The rate of production for the ith species in the jth reaction ($RoP_{i,j}$) is expressed as:

$$RoP_{i,j} = v_{i,j} r_j, \tag{8}$$

where $v_{i,j}$ and r_j are the stoichiometric coefficient of species i and the net reaction rate of reaction j, respectively. For reversible reaction, r_j can be positive or negative, depending on the dominant reaction direction. For a given species, a positive value of the production rate means that the species is generated and a negative one indicates consuming of the species. Based on the production rate of species, the ZND detonation reaction pathway can be established.

The heat release rate of the jth reaction (HRR_j) is defined as:

$$HRR_j = \Delta_r H_j^\circ r_j, \tag{9}$$

and the total heat release rate (HRR_t) is calculated by:

$$HRR_t = \sum_{j=1}^{291} HRR_j, \tag{10}$$

where $\Delta_r H_j^\circ$ is the standard reaction enthalpy of the reaction j. The total heat release of reaction j and the detonation process can be obtained by integrating Eq. (9) and Eq. (10), respectively. For the heat release rate and total heat release, a positive value indicates heat release, while a negative value means heat absorption. By judging the magnitude of these values, the main exothermic reactions and endothermic reactions in the ZND detonation can be determined.

The sensitivity coefficient of the *j*th reaction (Sen_j) is calculated by perturbing each reaction rate constant (k_j) by 1%, i.e.,

$$Sen_j = \frac{k_j}{P_r}\frac{\partial P_r}{\partial k_j} \approx 100\frac{P_r^+ - P_r}{P_r}, \tag{11}$$

where P_r and P_r^+ represent the parameter obtained before and after the perturbation of reaction rate constant, respectively. The induction length was selected to identify the reactions that hydrogen blend ratio has a greater influence. According to the definition, a reaction with a positive coefficient inhibits the reactivity and a negative one is beneficial for promoting the reactivity.

In addition, the rate of production, the heat release, and the sensitivity coefficient are normalized. The positive and negative values are summed separately, then the positive value is normalized with the sum of the positive ones and the negative value is normalized with the absolute value of the sum of the negative ones. The normalized values which are greater than 10% are considered in the subsequent results and discussion.

Results and discussion

ZND detonation structure

Figure 1 shows the temperature and pressure profiles of ZND detonation in stoichiometric CH_4-air mixture. ZND detonation structure consists of an unburned zone, an induction zone, a reaction zone, and a burned zone. Before the leading shock wave, which is at 0 mm position, is the (a) unburned zone, where the mixture with the initial temperature (T_0) of

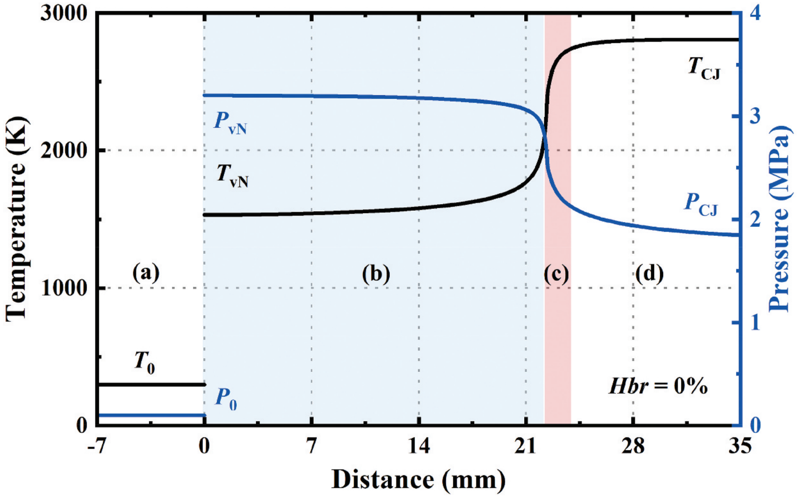

Figure 1. Temperature and pressure profiles of ZND detonation structure in stoichiometric CH_4-air mixture.

298 K and initial pressure (P_0) of 101,325 Pa. The leading shock wave adiabatically compresses and heats the reactants to the ignition temperature. Following the leading shock wave is the induction zone (i.e., zone b filled with blue), which is almost thermally neutral. Therefore, the thermodynamics state of the shock-heated mixture remains relatively constant (i.e., von Neumann temperature and pressure, T_{vN} and P_{vN}) through the induction zone. After the induction zone is the reaction zone (i.e., zone c filled with red). In the reaction zone, there is an increase in temperature and a decrease in pressure. For an unsupported detonation wave, the pressure decreases further in the expansion fan that trails behind the reaction zone. It is this expansion that accelerates the gases backward away from the front, which produces the forward thrust that supports the propagation of the leading shock wave. The pressure and temperature will reach Chapman-Jouguet (CJ) equilibrium in the (d) burned zone. The CJ detonation pressure and temperature (P_{CJ}, T_{CJ}), as well as von Neumann pressure and temperature (P_{vN}, T_{vN}) of stoichiometric CH_4 /H_2/air mixtures with different hydrogen blend ratios, are summarized in Table 1. The ranges of temperature and pressure for the mixture without hydrogen are 1532–2796 K and 1.75–3.20 MPa, respectively. As the hydrogen blend ratio increases from 0% to 100%, the temperature difference of mixture between CJ state and vN state increases by 12.50% while the pressure difference decreases by 14.48%.

According to prior research (Gimeno-Escobedo et al. 2019; Li et al. 2014; Wang et al. 2009) about the premixed laminar flame of CH_4-H_2 binary fuels, some typical species (e.g.,

Table 1. Steady ZND detonation properties of stoichiometric CH_4/H_2/air mixtures with different hydrogen blend ratios.

Hbr	P_{CJ} (MPa)	P_{vN} (MPa)	T_{CJ} (K)	T_{vN} (K)
0%	1.75	3.20	2796	1532
20%	1.73	3.17	2806	1533
50%	1.71	3.11	2830	1533
80%	1.65	2.98	2881	1535
100%	1.58	2.82	2960	1538

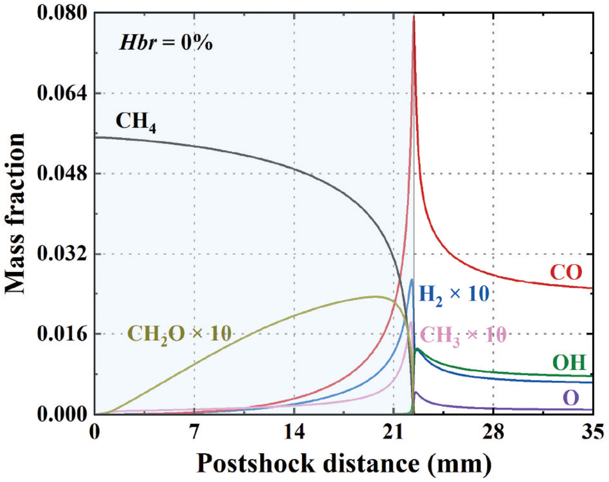

Figure 2. Species profiles of ZND detonation structure of stoichiometric CH_4-air mixture.

CH_4, CH_3, and H_2, etc.) are chosen to analyze the steady detonation structure. Figure 2 shows the species profiles of ZND detonation structure of stoichiometric CH_4-air mixture. The leading shock wave is at 0 mm position, and the induction zone (blue-filled area) of ZND detonation structure is behind the leading shock wave. In the induction zone, the active radical species are generated by the thermal dissociation of the shock-heated molecules. When sufficient concentrations of the active radical species are produced, rapid chain-branching reactions convert the reactants to products. The mass fraction of CH_4 decreases to 0 at the end of the induction region. The amount of CH_2O increases steadily and then decreases to 0 at a position close to the one of CH_4. The mass fractions of CH_3 and CO rise gradually, reaching a peak at the end of the induction zone. As for O and OH, their mass fractions increase at the position close to the end of the induction zone and decrease slightly until stabilized. The evolutions of the selected species indicate that CH_3, CH_2O, and CO are the important intermediate species during the detonation process of CH_4-air mixture, while CO, OH, H_2, and O are the main products.

The effect of adding hydrogen into stoichiometric CH_4-air mixture on the ZND steady detonation structure can be seen in Figure 3. For the cases with *Hbr* = 20%, 50%, and 80%, the mass fraction evolutions of CH_4, CH_3, CH_2O, CO, O, and OH are similar to the mixture without hydrogen addition. The main difference is that CH_2O in the mixtures with 50% and 80% *Hbr* show different growth trends, especially in the case containing 80% *Hbr*. There is hardly any CH_2O over a relatively long distance in the

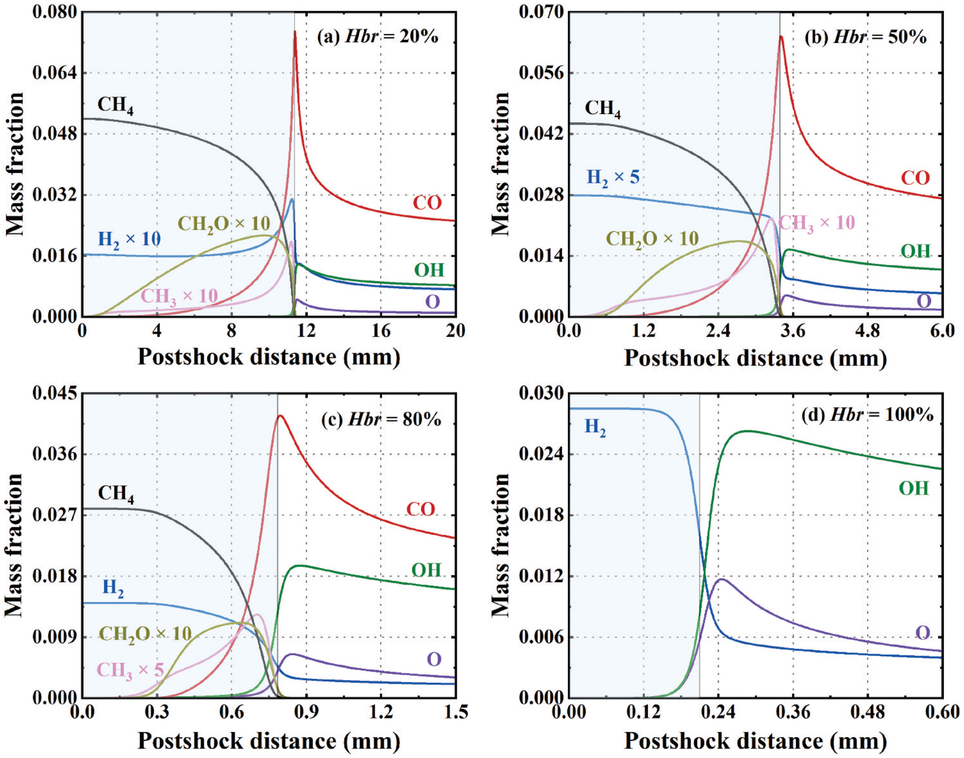

Figure 3. Species profiles of ZND detonation structure of stoichiometric CH_4/H_2/air mixtures with different hydrogen blend ratios, i.e., *Hbr* = (a) 20%, (b) 50%, (c) 80%, and (d) 100%.

induction zone. The slow increase of CH_2O mass fraction during the induction stage is more obvious with increasing hydrogen blend ratio. As for stoichiometric H_2-air mixture, the mass fractions of O and OH are more than the mixture with methane. In addition, the mass fraction of H_2 exhibits different evolution trends when the hydrogen blend ratio increases from 0% to 100%. When *Hbr* ≤ 20%, H_2 mass fraction increases and then decreases until stabilized, see Figures 2 and 3a. As shown in Figure 3b-d, the mass fraction of H_2 decreases and tends to be a constant for the cases with *Hbr* ≥ 50%. This indicates that in CH_4-H_2 binary fuels, the consumption of hydrogen surpasses its generated amount when the hydrogen blend ratio exceeds a critical value. The critical hydrogen blend ratio is 20%, which is in accordance with the study of Wang et al. (2009) on the laminar flame of CH_4/H_2/air mixtures.

Figure 4 shows the maximum mass fraction of selected species during ZND detonation of stoichiometric CH_4/H_2/air mixtures with different hydrogen blend ratios. With the increases of hydrogen addition, the mass fraction of CH_4 decreases and the mass fraction of H_2 increases, but the mass fraction of CH_3 increases. This can be contributed to the fact that adding hydrogen promotes the conversion of CH_4.

In order to explore the changing mechanisms of CH_2O, CH_3 and H_2 mass fractions in stoichiometric CH_4/H_2/air mixtures ZND detonation structures, the ZND detonation reaction pathways were established, as shown in Figure 5. For the pathway of C-reactions, CH_4 is converted to CO_2 in the following two routes:

Route 1: CH_4 => CH_3 => C_2H_6 => . . . => CO_2,
Route 2: CH_4 => CH_3 (=> CH_3O) => CH_2O => HCO => CO => CO_2.

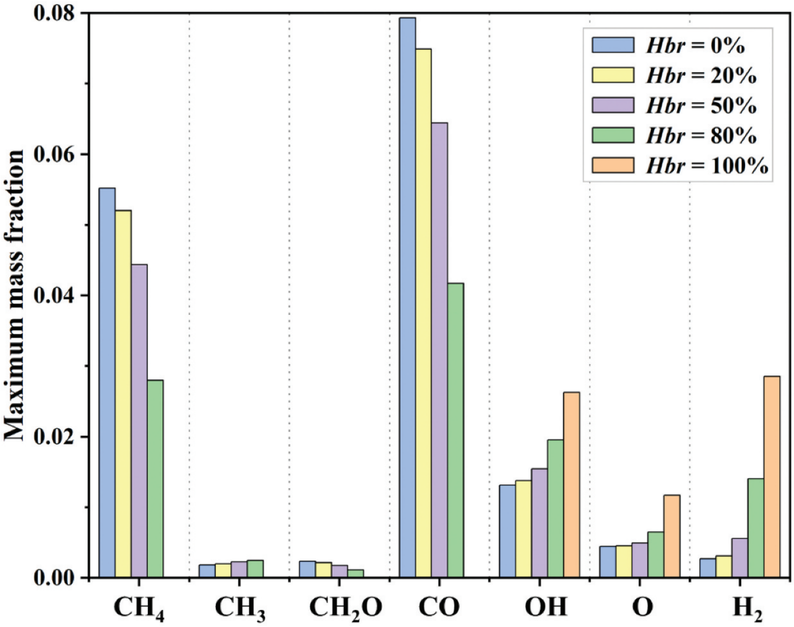

Figure 4. Maximum mass fraction of selected species during ZND detonation of stoichiometric CH_4/H_2/air mixtures with different hydrogen blend ratios.

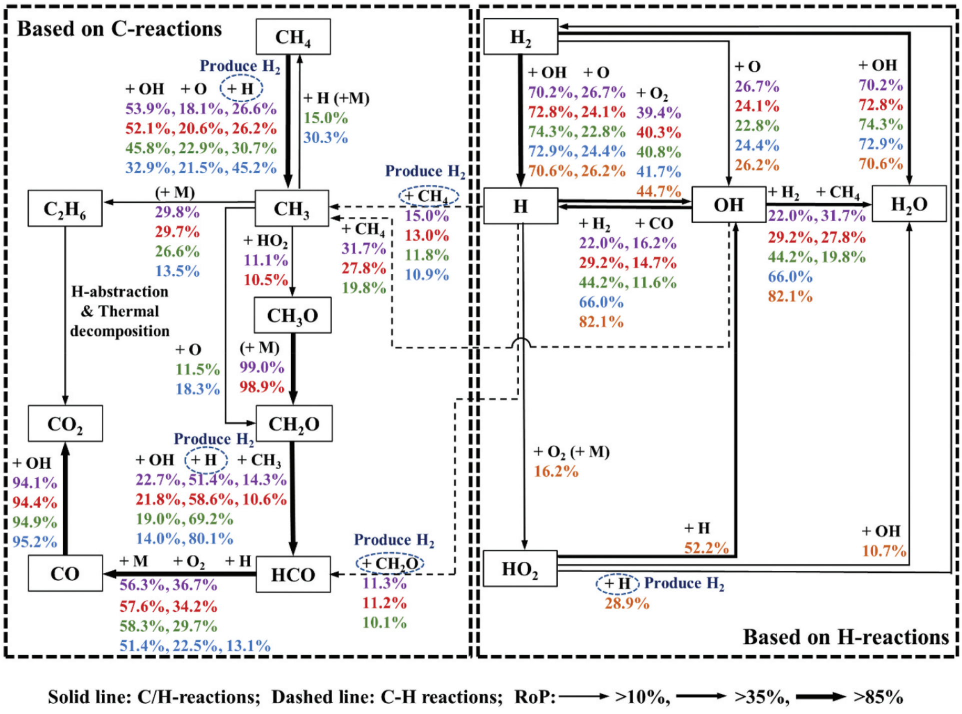

Figure 5. Reaction pathway analysis for stoichiometric CH_4/H_2/air mixtures with different hydrogen blend ratios based on C-reactions and H-reactions. The values are the absolute ones of the negative rate of production: purple, *Hbr* = 0%; red, *Hbr* = 20%; green, *Hbr* = 50%; blue, *Hbr* = 80% and brownness, *Hbr* = 100%.

The transformation process of C_2H_6 to CO_2 in route 1 is governed by H-abstraction and thermal decomposition (Xiao and Li 2022). In route 1, H_2 can be generated by CH_4 through R135 ($CH_4 + H <=> CH_3 + H_2$). The reaction producing H_2 in route 2 is R86: $CH_2O + H <=> HCO + H_2$. These two reactions result in the formation of hydrogen during the combustion of hydrocarbon fuels, as shown in Figures 2 and 3a. In addition, more than 95% of the spontaneously produced hydrogen reacts with either OH or O to form H. The production of H provides a certain source of hydrogen (10%-35%) for R135 and R86. However, more than 35% of H reacts with O_2 to produce OH, which is eventually converted to H_2O (see H-reactions).

In the cases of hydrogen blend ratio from 0% to 80%, route 1 is one of the main ZND detonation reaction pathways of stoichiometric CH_4/H_2/air mixtures. When *Hbr* = 0%, 20%, 50%, and 80%, the conversion rate of CH_4 to CH_3 is 98.6%, 98.9%, 99.4%, and 99.65%, respectively, showing an increasing trend (see Figure 4). This reaction pathway indicates that R135 ($CH_4 + H <=> CH_3 + H_2$) plays the key role in facilitating the chemical reaction. Adding H_2 produces more H and promotes the forward reaction of R135, increasing the production of H_2 and forming the positive feedback. For the cases with *Hbr* = 0% and 20%, route 2 is $CH_4 => CH_3 => CH_3O => CH_2O => HCO => CO => CO_2$. When *Hbr* increases to 50% and 80%, after CH_4 is converted to CH_3, part of CH_3 is converted to CH_2O by reacting with O (i.e., R97: $CH_3 + O <=> CH_2O + H$) without forming the intermediate product CH_3O. This change in the pathway results in different evolutions of CH_3 and CH_2O in the mixtures containing 50% and 80% hydrogen (see Figures 2 and 3). When the hydrogen blend ratio increases to 100%, there are two main reaction pathways for the ZND detonation, which can be seen in H-reactions:

Route 3: H_2 => H => HO_2 (=> OH) => H_2O,
Route 4: H_2 (=> H) => OH => H_2O.

Induction length

The induction length (Δ_I) is an important detonation characteristic, which is of great significance to the prediction of detonation limit (e.g., detonation cell size and critical pressure). It is defined as the distance from the leading shock wave to the maximum thermicity. Figure 6 shows the thermicity profiles of ZND detonation of stoichiometric CH_4/H_2/air mixtures with different hydrogen blend ratios. The maximum thermicity and induction length are influenced by hydrogen blend ratios evidently. For the mixtures with *Hbr* = 0%, 20%, 50%, 80%, and 100%, the induction length is 22.35, 11.32, 3.35, 0.75, and 0.21 mm, respectively. When the hydrogen blend ratio increases from 0% to 100%, the induction length decreases with a 99.06% decrement.

Since the induction length is the characteristic length measuring the heat release zone based on the chemical dynamics (Lee 2008), the normalized heat release of main reactions during the ZND detonation process in stoichiometric CH_4/H_2/air mixtures with various hydrogen blend ratios was shown in Figure 7. It is found that R0, R34, and R237 are important to the total heat absorption in stoichiometric CH_4-air mixture. After adding hydrogen to the mixture, R0 is influenced considerably. When *Hbr* = 100%, the heat absorbed by R0 accounts for 90% of the total heat absorption.

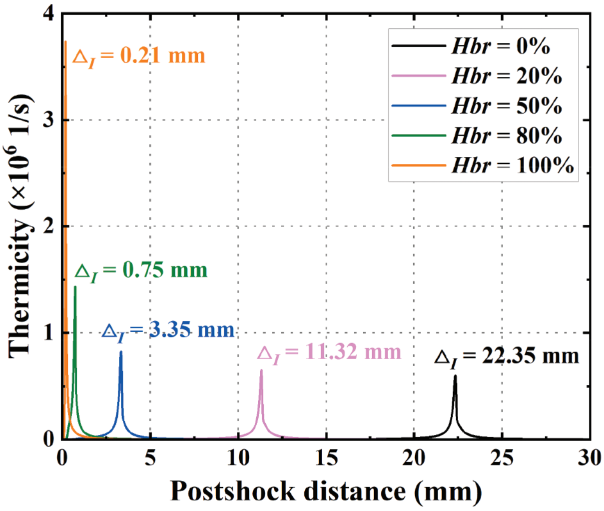

Figure 6. Thermicity profiles of ZND detonation of stoichiometric CH_4/H_2/air mixtures with various hydrogen blend ratios.

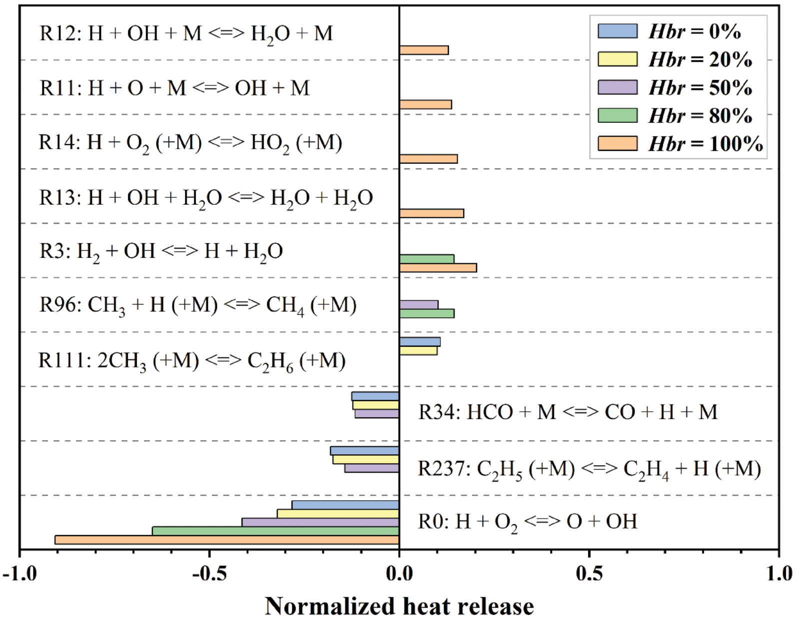

Figure 7. Normalized heat release of main reactions in stoichiometric CH_4/H_2/air mixtures with different hydrogen blend ratios.

Further analysis focuses on the change of the heat release rate with the postshock distance aside from the investigation on the dominant reactions. Figure 8a shows the heat release rate by different reactions for the ZND detonation of stoichiometric CH_4-air mixture. The heat release rate of exothermic reaction (R111) is reduced to 0 after the induction phase, which is related to the distribution of CH_3 (see Figure 2). For the main endothermic reactions (R0 and R34), the heat release rates reach the peak at the end of the induction zone. Figure 8b-e shows the heat release rate of the main reactions as a function of postshock distance for the stoichiometric CH_4/H_2/air mixtures with (b) 20%, (c) 50%, (d) 80% and (e) 100% *Hbr*. In the mixture with *Hbr* = 20%, all the heat release rates evolutions of the main reactions are similar to the mixture without hydrogen addition. The main difference is the peak values of heat release rate. For the cases with *Hbr* = 50%, 80%, and 100%, the maximum heat release rates of all the exothermic reactions and the main endothermic reaction (R0) increase significantly with rising the hydrogen blend ratio. This indicates that R0 is the most important reaction governing the heat release during the ZND detonation. Adding hydrogen promotes the heat release of R0 and enhances the energy absorption during induction phase, thereby making the molecular thermal decomposition after leading shock wave easier (Lee 2008) and leading to the decrease of induction length.

To explore whether R0 is the most important reaction affecting the induction length, the sensitivity analysis of the induction length was conducted. Figure 9 shows the normalized sensitivity of induction length to reaction rate constant for ZND detonation of stoichiometric CH_4/H_2/air mixtures with various hydrogen blend ratios. According to the definition in thermo-chemical analysis, the reactions with a negative normalized sensitivity (i.e., R0, R3, R104, and R106) are beneficial for promoting the reactivity of mixtures. The

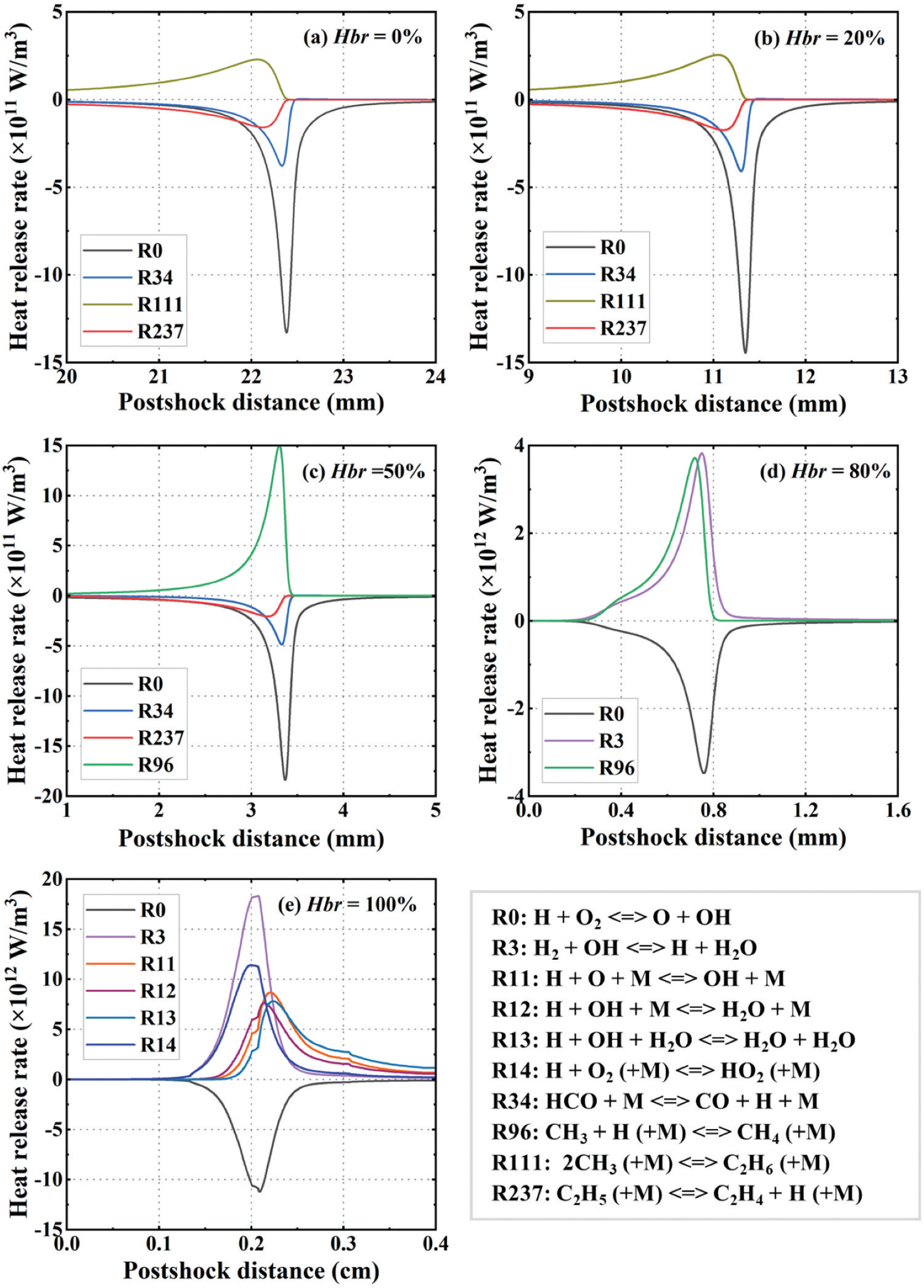

Figure 8. Heat release rate by different reactions for ZND detonation of stoichiometric CH_4/H_2/air mixtures with (a) 0%, (b) 20%, (c) 50%, (d) 80%, and (e) 100% *Hbr* as a function of postshock distance.

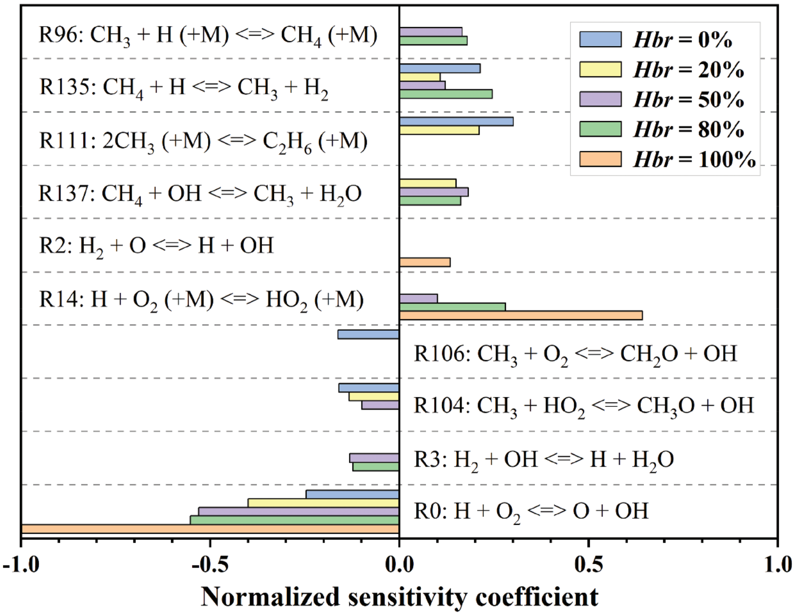

Figure 9. Normalized sensitivity of induction length to reaction rate constant for ZND detonation of stoichiometric CH_4/H_2/air mixtures with different hydrogen blend ratios.

normalized sensitivity of R0 is influenced by hydrogen blending more significantly compared with those of R3, R104, and R106. As for the normalized sensitivity of R0, it becomes smaller with the increasing hydrogen blend ratio. This shows that with the increase of hydrogen blend ratio, R0 has a stronger promoting effect on the reactivity of mixtures. This further proves that R0 controls the main heat release during the ZND detonation, and causes a decrease in induction length with increasing hydrogen blend ratio.

Detonation cell size

Detonation cell size is a basic parameter to characterize the detonation behaviors. Figure 10 shows the detonation cell size of stoichiometric CH_4/H_2/air mixtures. The data in Figure 10 includes two parts. One part is calculated initially at 298 K and 101,325 Pa through the prediction model of detonation cell size proposed by Westbrook et al. (1983), Gavrikov et al. (2000), Ng et al. (2007), and Lu et al. (2021). These prediction models of detonation cell size (λ) are summarized in Table 2, and the coefficients in the models proposed by Gavrikov et al. (2000) and Ng et al. (2007) can be found in their prior research. In addition, the detonation stability parameter χ, which measures the stability of detonation, is defined as (Ng et al. 2005):

$$\chi \equiv \varepsilon_{\mathrm{I}} \frac{\Delta_{\mathrm{I}}}{\Delta_{\mathrm{R}}} = \varepsilon_{\mathrm{I}} \Delta_{\mathrm{I}} \frac{\dot{\sigma}_{\max}}{\mathrm{u}_{CJ}}, \tag{12}$$

where Δ_R is the reaction length, and ε_I is the effective activation energy during the induction process. The reaction length is estimated by the ratio of the particle velocity at the CJ plane (u_{CJ}) to the maximum thermicity ($\dot{\sigma}_{\max}$) in the shock-attached frame. The effective

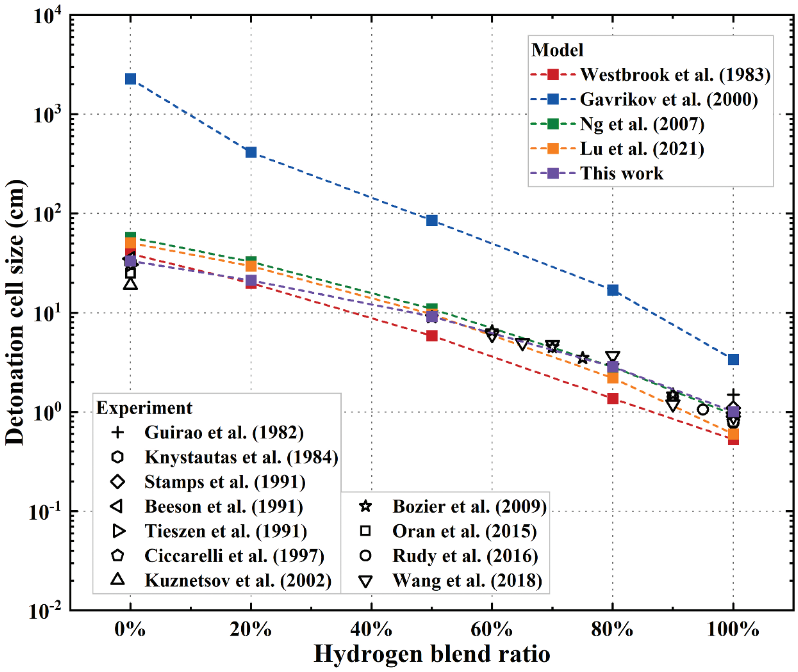

Figure 10. Detonation cell size of stoichiometric CH_4/H_2/air mixtures with various hydrogen blend ratios.

Table 2. Prediction model of detonation cell size.

Author	Prediction model
Westbrook et al.	$\lambda = 29_I$
Gavrikov et al.	$lg\left(\frac{\lambda}{I}\right) = \frac{T_{vN}}{T_0}\left(a\frac{T_{vN}}{T_o} - b\right) + \varepsilon_I\left[c\varepsilon_I - d + \left(e - f\frac{T_{vN}}{T_o}\right)\frac{T_{vN}}{T_0}\right] + g\ln\left(\frac{T_{vN}}{T_o}\right) + h\ln(\varepsilon_I) + \frac{T_{vN}}{T_o}\left(\frac{i}{\varepsilon_I} - \frac{k}{\varepsilon_I^m}\frac{T_{vN}}{T_o}\right) - j$
Ng et al.	$\lambda = A(x)_I = \sum_{i=1}^{n}(a_i x^{-i} + b_i x^i)_I = \left[A_o + \left(\frac{a_n}{x^n} + \ldots\ldots + \frac{a_1}{x^1} + b_1 x^1 + \ldots\ldots + b_n x^n\right)\right]_I$
Lu et al.	$\lambda = \left(-5.34 \times 10^{-4}\varepsilon_I^4 + 3.63 \times 10^{-2}\varepsilon_I^3 - 9.41 \times 10^{-1}\varepsilon_I^2 + 8.96\varepsilon_I + 2.81\right)_I$
This work	$\lambda = A(x)_I = \left(10^{1.89242}x^{-0.31696}\right)_I$

activation energy can be obtained by running two calculations of the constant-volume explosion with initial conditions (T_1,τ_1) and $(T_2,\ \tau_2)$:

$$\varepsilon_I = \frac{E_a}{RT_{vN}} = \frac{1}{T_{vN}}\left(\frac{\ln\tau_2 - \ln\tau_1}{1/T_2 - 1/T_1}\right), \tag{13}$$

where τ is the induction time.

Another part is the experimental data picked up from Ref (Bozier et al. 2009; Oran, Gamezo, and Zipf 2015; Rudy, Zbikowski, and Teodorczyk 2016; Wang et al. 2018) and the Detonation Database (Kaneshige and Shepherd 1997). These experiments are conducted initially at 293–300 K and 100–101.5 kPa. It is shown that all the detonation cell sizes become smaller with the increase of hydrogen blend ratio, due to the decrement of the induction length. As for the predictions by the models, the results calculated by the model of Ng et al. (2007) are relatively more consistent with the experimental measurements on the

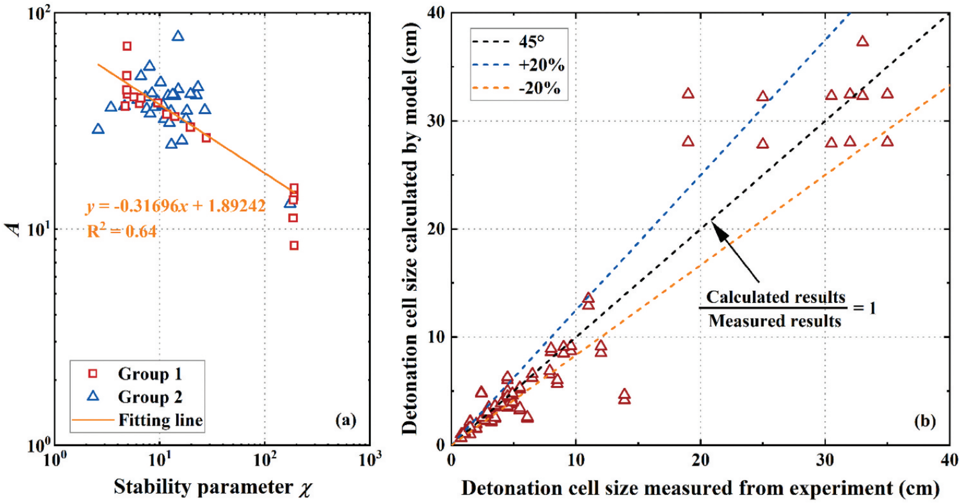

Figure 11. (a) Evolution of *A* with stability parameter χ, and (b) comparison of measured and calculated values of detonation cell size in CH_4/H_2/air mixtures.

whole, especially compared with Gavrikov's, Gavrikov et al. (2000). However, the prediction model developed by Ng et al. (2007) significantly overestimates the detonation cell size of the cases with low hydrogen blend ratio ($Hbr = 0\%$) for CH_4/H_2/air mixtures.

In this context, we develop a detonation cell size prediction model for CH_4/H_2/air mixtures based on the prediction model proposed by Ng et al. (2007). In Ng model, the detonation cell sizes can be calculated as $\lambda = A(\chi)\Delta_I$. Since the induction length is constant for a certain mixture, the relationship between the coefficient A and stability parameter χ is plotted in Figure 11a to investigate the trend of $A(\chi)$. The data in group 1 are the experimental data of detonation cell size in Figure 10. The data in group 2 come from the experiments (Bozier et al. 2009; Kaneshige and Shepherd 1997) and the equivalent ratio, initial pressure, and initial temperature range from 0.5–2.5, 25.5–151.3 kPa, and 293–300 K, respectively in these experiments. These initial conditions differ relatively large compared with those in this study. The stability parameters in Figure 11a are calculated using FFCM-1 mechanism. The coefficient A is obtained by dividing the measured detonation cell size by the calculated induction length. The evolution of $A(\chi)$ can be determined by fitting the data in Figure 11a. Finally, the detonation cell size prediction model for CH_4/H_2/air mixtures can be expressed as:

$$\lambda = A(\chi)\Delta_I = \left(10^{1.89242}\chi^{-0.31696}\right)\Delta_I. \tag{14}$$

This prediction model is also added in Table 2 for comparison with other models.

Figure 11b shows the comparison between the measured values of the detonation cell size and the calculation results using Eq. (14). When the calculated detonation cell size is equal to the experimental measurement, the data is located on the 45° line in Figure 11b. In addition, a range of prediction accuracy of ± 20% is plotted. It is notable that the calculated detonation cell sizes using the prediction model are close to the measurements, which can be seen in Figures 10–11. The error can be controlled within ± 20% for most detonation cell size predictions of CH_4/H_2/air mixtures, especially for large ones.

Conclusions

The ZND detonations of stoichiometric CH_4/H_2/air mixtures were explored numerically in this paper, which can be helpful for understanding the ZND detonation structure and characteristics of CH_4-H_2 binary fuels. Different hydrogen blend ratios were selected to explore the effect of hydrogen on the ZND detonation structure and the detonation characteristics (induction length and detonation cell size) by steady 1D ZND calculation and thermo-chemical analysis.

The results show that hydrogen plays a significant role on the ZND reaction pathway of CH_4/H_2/air mixture. When $Hbr \leq 20\%$, CH_4 is converted to CO_2 by route 1: CH_4 => CH_3 => C_2H_6 => … => CO_2 and route 2: CH_4 => CH_3 => CH_3O => CH_2O => HCO => CO => CO_2. When $Hbr \geq 50\%$, CH_3 in route 2 is directly converted to CH_2O through R97 ($CH_3 + O <=> CH_2O + H$). This leads to different growth trends of the mass fractions of CH_3 and CH_2O in the mixtures with 50% and 80% *Hbr* in the ZND detonation structures compared with those for $Hbr \leq 20\%$. Interestingly, hydrogen was found can be generated by R135, R86, and R15 in stoichiometric CH_4/H_2/air mixtures during the detonation process. R135 ($CH_4 + H <=> CH_3 + H_2$) is the most important reaction in facilitating the conversion of CH_4 to CH_3.

The induction length decreases significantly as the hydrogen blend ratio increases. The thermal-chemical analysis indicates that the endothermic reaction (R0: $H + O_2 <=> O + OH$) governs the decrease of induction length. Increasing the hydrogen proportion in stoichiometric CH_4/H_2/air mixtures enhances the heat release of R0 during the induction stage. This is favorable to the absorption of energy and the molecular thermal decomposition after the leading shock wave.

In the mixtures of stoichiometric CH_4/H_2/air, the detonation cell size decreases with the increase of hydrogen blend ratio. A prediction model of detonation cell size incorporated with detonation stability parameter and induction length, $\lambda = A(\chi)\Delta_I = (10^{1.89242}\chi^{-0.31696})\Delta_I$, was developed for CH_4/H_2/air mixtures. The prediction results obtained by using this model show a good agreement with the prior experimental measurements. In the future, the impact of initial pressure on the structure and characteristics of ZND detonation in CH_4/H_2/air mixtures still needs to be explored.

Disclosure statement

No potential conflict of interest was reported by the author(s).

Funding

This study was supported by the National Natural Science Foundation of China [Nos. 12302449 and 52104227], the Anhui Provincial Natural Science Foundation [No. 2308085QE170], and the Fundamental Research Funds for the Central Universities [No. WK2320000055].

References

Bozier, O., R. Sorin, F. Virot, R. Zitoun, and D. Desbordes. 2009. Detonability of binary H_2/CH_4/AIR mixtures. International Conference on Hydrogen Safety, Ajaccio, France.

Browne, S., J. Ziegler, N. Bitter, B. Schmidt, J. Lawson, and J. Shepherd. 2018. SDToolbox: Numerical tools for shock and detonation wave modeling. https://shepherd.caltech.edu/EDL/PublicResources/sdt/.

Cai, C., M. Li, J. Dong, and H. Xiao. 2023. Flame acceleration in stoichiometric CH_4/H_2/air mixtures with different hydrogen blend ratios in an obstructed channel. *Combust. Sci. Technol.* 1–20. doi:10.1080/00102202.2023.2203819.

Cai, P., Z. Liu, P. Li, Y. Zhao, M. Li, R. Li, C. Wang, and Z. Xiu. 2022. Effects of fuel component, airflow field and obstacles on explosion characteristics of hydrogen/methane mixtures fuel. *Energy* 265:126302. doi:10.1016/j.energy.2022.126302.

Chaumeix, N., S. Pichon, F. Lafosse, and C. E. Paillard. 2007. Role of chemical kinetics on the detonation properties of hydrogen/natural gas/air mixtures. *Int. J. Hydrog. Energy.* 32 (13):2216–26. doi:10.1016/j.ijhydene.2007.04.008.

Cheng, Y., C. Tang, Z. Huang. 2015. Kinetic analysis of H_2 addition effect on the laminar flame parameters of the C1–C4 n-alkane-air mixtures: From one step overall assumption to detailed reaction mechanism. *Int. J. Hydrog. Energy.* 40 (1):703–18. doi:10.1016/j.ijhydene.2014.11.010.

de Goey, L. P. H., R. T. E. Hermanns, and R. J. M. Bastiaans. 2007. Analysis of the asymptotic structure of stoichiometric premixed CH4–H2–air flames. *Proc. Combust. Inst.* 31 (1):1031–38. doi:10.1016/j.proci.2006.07.072.

Gavrikov, A. I., A. A. Efimenko, and S. B. Dorofeev. 2000. A model for detonation cell size prediction from chemical kinetics. *Combust. Flame.* 120 (1):19–33. doi:10.1016/S0010-2180(99)00076-0.

Gimeno-Escobedo, E., A. Cubero, J. S. Ochoa, and N. Fueyo. 2019. A reduced mechanism for the prediction of methane-hydrogen flames in cooktop burners. *Int. J. Hydrog. Energy.* 44 (49):27123–40. doi:10.1016/j.ijhydene.2019.08.165.

Goodwin, D. G., H. K. Moffat, I. Schoegl, R. L. Speth, and B. W. Weber. 2022. Cantera: An object-oriented software toolkit for chemical kinetics, thermodynamics, and transport processes (2.6.0). doi:10.5281/zenodo.6387882.

He, Y., M. Liang, S. Liao, X. Jian, Y. Shao, and Z. Jin. 2020. Chemical effects of hydrogen addition on low-temperature oxidation of premixed laminar methane/air flames. *Fuel* 280:118600. doi:10.1016/j.fuel.2020.118600.

Huang, Z., Y. Zhang, K. Zeng, B. Liu, Q. Wang, and D. Jiang. 2006. Measurements of laminar burning velocities for natural gas–hydrogen–air mixtures. *Combust. Flame* 146 (1–2):302–11. doi:10.1016/j.combustflame.2006.03.003.

Kaneshige, M., and J. E. Shepherd. 1997. Detonation database. *Mol. Endocrinol. (Baltim. Md.)* 11 (11):1747–55. doi:10.1210/mend.11.11.0012.

Kumar, D. S., K. Ivin, and A. V. Singh. 2021. Sensitizing gaseous detonations for hydrogen/ethylene-air mixtures using ozone and H_2O_2 as dopants for application in rotating detonation engines. *Proc. Combust. Inst.* 38 (3):3825–34. doi:10.1016/j.proci.2020.08.061.

Lee, J. H. 2008. *The detonation phenomenon*. Cambridge: Cambridge University Press.

Li, H., and H. Xiao. 2023a. Effect of H_2 addition on laminar burning velocity of NH_3/DME blends by experimental and numerical method using a reduced mechanism. *Combust. Flame.* 257:113000. doi:10.1016/j.combustflame.2023.113000.

Li, H., and H. Xiao. 2023b. Experimental study on the explosion characteristics of NH_3/DME/air mixtures. *Fuel* 352:129069. doi:10.1016/j.fuel.2023.129069.

Li, H., H. Xiao, and J. Sun. 2022. Laminar burning velocity, Markstein length, and cellular instability of spherically propagating NH_3/H_2/Air premixed flames at moderate pressures. *Combust. Flame.* 241:112079. doi:10.1016/j.combustflame.2022.112079.

Li, Q., G. Hu, S. Liao, Q. Cheng, C. Zhang, and C. Yuan. 2014. Kinetic effects of hydrogen addition on the thermal characteristics of methane–air premixed flames. *Energy Fuels* 28 (6):4118–29. doi:10.1021/ef500263v.

Li, Q., Z. Wei, Z. Lv, W. Guo, and X. Liu. 2022. The behaviors of supersonic combustion wave through a perforated plate in a stoichiometric mixtures of $H_2/CH_4/O_2$ and H_2/O_2. *Fuel* 317:123092. doi:10.1016/j.fuel.2021.123092.

Li, T., F. Hampp, and R. Lindstedt. 2015. Turbulent explosions in H_2 enriched CO and CH_4 mixtures. Proceedings of the 25th ICDERS, Leeds, UK.

Li, Z., Z. Weng, and R. Mével. 2022. Thermo-chemical analyses of steady detonation wave using the shock and detonation toolbox in Cantera. *Shock Waves* 32 (8):759–62. doi:10.1007/s00193-022-01107-0.

Liu, L., Z. Luo, T. Wang, F. Cheng, S. Gao, and H. Liang. 2021. Effects of initial temperature on the deflagration characteristics and flame propagation behaviors of CH_4 and its blends with C_2H_6, C_2H_4, CO, and H_2. *Energy Fuels* 35 (1):785–95. doi:10.1021/acs.energyfuels.0c03506.

Lu, X., C. R. Kaplan, and E. S. Oran. 2021. A chemical-diffusive model for simulating detonative combustion with constrained detonation cell sizes. *Combust. Flame* 230:111417. doi:10.1016/j.combustflame.2021.111417.

Mejía-Botero, C. C., F. Veiga-López, and J. Melguizo-Gavilanes. 2022. Minimum tube diameters for detonation propagation in CH_4/H_2-air mixtures: Implications for natural gas cooktop burners. *J. Loss Prev. Process Ind.* 80:104919. doi:10.1016/j.jlp.2022.104919.

Midilli, A., M. Ay, I. Dincer, and M. A. Rosen. 2005. On hydrogen and hydrogen energy strategies: I: Current status and needs. *Renewable Sustain. Energy Rev.* 9 (3):255–71. doi:10.1016/j.rser.2004.05.003.

Mitu, M., V. Giurcan, D. Razus, and D. Oancea. 2020. Influence of initial pressure and vessel's geometry on deflagration of stoichiometric methane–air mixture in small-scale closed vessels. *Energy Fuels* 34 (3):3828–35. doi:10.1021/acs.energyfuels.9b04450.

Ng, H. D., Y. Ju, and J. H. Lee. 2007. Assessment of detonation hazards in high-pressure hydrogen storage from chemical sensitivity analysis. *Int. J. Hydrog. Energy.* 32 (1):93–99. doi:10.1016/j.ijhydene.2006.03.012.

Ng, H. D., and J. H. S. Lee. 2008. Comments on explosion problems for hydrogen safety. *J. Loss Prev. Process Ind.* 21 (2):136–46. doi:10.1016/j.jlp.2007.06.001.

Ng, H. D., M. I. Radulescu, A. J. Higgins, N. Nikiforakis, and J. H. S. Lee. 2005. Numerical investigation of the instability for one-dimensional Chapman–jouguet detonations with chain-branching kinetics. *Combust. Theory Model.* 9 (3):385–401. doi:10.1080/13647830500307758.

Ogden, J., A. M. Jaffe, D. Scheitrum, Z. McDonald, and M. Miller. 2018. Natural gas as a bridge to hydrogen transportation fuel: Insights from the literature. *Energy Policy* 115:317–29. doi:10.1016/j.enpol.2017.12.049.

Okafor, E. C., Y. Naito, S. Colson, A. Ichikawa, T. Kudo, A. Hayakawa, and H. Kobayashi. 2018. Experimental and numerical study of the laminar burning velocity of CH_4–NH_3–air premixed flames. *Combust. Flame* 187:185–98. doi:10.1016/j.combustflame.2017.09.002.

Oran, E. S., V. N. Gamezo, and R. K. Zipf. 2015. Large-scale experiments and absolute detonability of methane/air mixtures. *Combust. Sci. Technol.* 187 (1–2):324–41. doi:10.1080/00102202.2014.976308.

Pio, G., and E. Salzano. 2018. Laminar burning velocity of methane, hydrogen, and their mixtures at extremely low-temperature conditions. *Energy Fuels* 32 (8):8830–36. doi:10.1021/acs.energyfuels.8b01796.

Porowski, R., and A. Teodorczyk. 2013. Experimental study on DDT for hydrogen-methane-air mixtures in tube with obstacles. *J. Loss Prev. Process Ind.* 26 (2):374–79. doi:10.1016/j.jlp.2012.06.004.

Rodriguez, V., V. Monnier, P. Vidal, and R. Zitoun. 2022. Non-dimensionalized distances and limits for the transition of deflagration to detonation. *Shock Waves* 32 (5):417–25. doi:10.1007/s00193-022-01088-0.

Rudy, W., M. Zbikowski, and A. Teodorczyk. 2016. Detonations in hydrogen-methane-air mixtures in semi confined flat channels. *Energy* 116:1479–83. doi:10.1016/j.energy.2016.06.001.

Shamshin, I. O., M. V. Kazachenko, S. M. Frolov, and V. Y. Basevich. 2021. Deflagration-to-detonation transition in stochiometric mixtures of the binary methane-hydrogen fuel with air. *Int. J. Hydrog. Energy.* 46 (68):34046–58. doi:10.1016/j.ijhydene.2021.07.209.

Sher, E., and S. Refael. 1988. A simplified reaction scheme for the combustion of hydrogen enriched methane/air flame. *Combust. Sci. Technol.* 59 (4–6):371–89. doi:10.1080/00102208808947106.

Sorin, R., O. Bozier, R. Zitoun, and D. Desbordes. 2009. Deflagration to detonation transition in binary fuels H_2/CH_4 with air mixtures. Proceedings of the 22nd ICDERS, Minsk, Belarus.

Su, B., Z. Luo, T. Wang, C. Xie, and F. Cheng. 2021. Chemical kinetic behaviors at the chain initiation stage of CH_4/H_2/air mixture. *J. Hazard. Mater.* 403:123680. doi:10.1016/j.jhazmat.2020.123680.

Sun, J., B. Tian, and Z. Chen. 2022. Effect of ozone addition and ozonolysis reaction on the detonation properties of C_2H_4/O_2/Ar mixtures. *Proc. Combust. Inst.* 39 (3):2797–806. doi:10.1016/j.proci.2022.09.029.

Sun, X., and S. Lu. 2020a. Experimental study of detonation limits in CH_4-$2H_2$-$3O_2$ mixtures: Effect of different geometric constrictions. *Process Saf. Environ. Protect.* 142:56–62. doi:10.1016/j.psep.2020.06.002.

Sun, X., and S. Lu. 2020b. Experimental study on the detonation initiation using pipe bundle geometries in CH_4–$2H_2$–$3O_2$ mixture. *Energy* 199:117468. doi:10.1016/j.energy.2020.117468.

Takita, K., and T. Niioka. 1996. On detonation behavior of mixed fuels. *Shock Waves* 6 (2):61–66. doi:10.1007/BF02515188.

Tao, Y., G. P. Smith, and H. Wang. 2018. Critical kinetic uncertainties in modeling hydrogen/carbon monoxide, methane, methanol, formaldehyde, and ethylene combustion. *Combust. Flame* 195:18–29. doi:10.1016/j.combustflame.2018.02.006.

Wang, J., Z. Huang, C. Tang, H. Miao, and X. Wang. 2009. Numerical study of the effect of hydrogen addition on methane–air mixtures combustion. *Int. J. Hydrog. Energy.* 34 (2):1084–96. doi:10.1016/j.ijhydene.2008.11.010.

Wang, L. Q., H. H. Ma, Z. W. Shen, and D. G. Chen. 2018. Experimental study of DDT in hydrogen-methane-air mixtures in a tube filled with square orifice plates. *Process Saf. Environ. Protect.* 116:228–34. doi:10.1016/j.psep.2018.01.017.

Weng, Z. F., and R. Mevel. 2022. Real gas effect on steady planar detonation and uncertainty quantification. *Combust. Flame* 245:13. doi:10.1016/j.combustflame.2022.112318.

Weng, Z., R. Mével, and N. Chaumeix. 2023. Detonation in ammonia-oxygen and ammonia-nitrous oxide mixtures. *Combust. Flame* 251:112680. doi:10.1016/j.combustflame.2023.112680.

Weng, Z., F. Veiga-López, J. Melguizo-Gavilanes, and R. Mével. 2023. Effect of ozone addition on curved detonations. *Combust. Flame* 247:112479. doi:10.1016/j.combustflame.2022.112479.

Westbrook, C. K., and P. A. Urtiew. 1983. Use of chemical kinetics to predict critical parameters of gaseous detonations. *Combust. Explos. Shock Waves* 19 (6):753–66. doi:10.1007/BF00750785.

Xiao, H. H., Q. L. Duan, and J. H. Sun. 2018. Premixed flame propagation in hydrogen explosions. *Renew. Sust. Energ. Rev.* 81:1988–2001. doi:10.1016/j.rser.2017.06.008.

Xiao, H., and H. Li. 2022. Experimental and kinetic modeling study of the laminar burning velocity of NH_3/DME/air premixed flames. *Combust. Flame* 245:112372. doi:10.1016/j.combustflame.2022.112372.

Yu, G., C. Law, and C. Wu. 1986. Laminar flame speeds of hydrocarbon + air mixtures with hydrogen addition. *Combust. Flame* 63 (3):339–47. doi:10.1016/0010-2180(86)90003-9.

Zhang, B. 2019. Detonation limits in methane-hydrogen-oxygen mixtures: Dominant effect of induction length. *Int. J. Hydrog. Energy.* 44 (41):23532–37. doi:10.1016/j.ijhydene.2019.07.053.

Zhang, B., L. Pang, and Y. Gao. 2016. Detonation limits in binary fuel blends of methane/hydrogen mixtures. *Fuel* 168:27–33. doi:10.1016/j.fuel.2015.11.073.

Zhang, K., G. Hu, S. Liao, Z. Zuo, H. Li, Q. Cheng, and C. Xiang. 2016. Numerical study on the effects of oxygen enrichment on methane/air flames. *Fuel* 176:93–101. doi:10.1016/j.fuel.2016.02.064.